Inorganic Chemistry

Article

pubs.acs.org/IC

Anticancer Activity of Polyoxometalate-Bisphosphonate Complexes: Synthesis, Characterization, In Vitro and In Vivo Results

Amandine Boulmier,[†] Xinxin Feng,[‖] Olivier Oms,[†] Pierre Mialane,[†] Eric Rivière,[⊥] Christopher J. Shin,[‖] Jiaqi Yao,[‖] Tadahiko Kubo,[§] Taisuke Furuta,[§] Eric Oldfield,*[,‡,‖] and Anne Dolbecq*[,†]

[†]Institut Lavoisier de Versailles, UMR 8180, Université de Versailles Saint-Quentin en Yvelines, Université Paris-Saclay, 45 Avenue des Etats-Unis, 78035 Versailles Cedex, France

[‖]Department of Chemistry, University of Illinois at Urbana−Champaign, 600 South Mathews Avenue, Urbana, Illinois 6180, United States

[‡]Center for Biophysics and Quantitative Biology, University of Illinois at Urbana−Champaign, 1110 W Green Street, Urbana, Illinois 61801, United States

[§]Department of Orthopedic Surgery, Graduate School of Biomedical Sciences, Hiroshima University, Hiroshima, Japan

[⊥]Institut de Chimie Moléculaire et des Matériaux d'Orsay, UMR 8182, Université Paris-Sud, Université Paris-Saclay, 91405 Orsay, France

Supporting Information

ABSTRACT: We synthesized a series of polyoxometalate-bisphosphonate complexes containing $Mo^{VI}O_6$ octahedra, zoledronate, or an *N*-alkyl (*n*-C_6 or *n*-C_8) zoledronate analogue, and in two cases, Mn as a heterometal. Mo_6L_2 (L = Zol, $ZolC_6$, $ZolC_8$) and Mo_4L_2Mn (L = Zol, $ZolC_8$) were characterized by using single-crystal X-ray crystallography and/or IR spectroscopy, elemental and energy dispersive X-ray analysis and ^{31}P NMR. We found promising activity against human nonsmall cell lung cancer (NCI-H460) cells with IC_{50} values for growth inhibition of ~5 μM per bisphosphonate ligand. The effects of bisphosphonate complexation on IC_{50} decreased with increasing bisphosphonate chain length: $C_0 \approx 6.1\times$, $C_6 \approx 3.4\times$, and $C_8 \approx 1.1\times$. We then determined the activity of one of the most potent compounds in the series, $Mo_4Zol_2Mn(III)$, against SK-ES-1 sarcoma cells in a mouse xenograft system finding a ~5× decrease in tumor volume than found with the parent compound zoledronate at the same compound dosing (5 μg/mouse). Overall, the results are of interest since we show for the first time that heteropolyoxomolybdate-bisphosphonate hybrids kill tumor cells in vitro and significantly decrease tumor growth, in vivo, opening up new possibilities for targeting both Ras as well as epidermal growth factor receptor driven cancers.

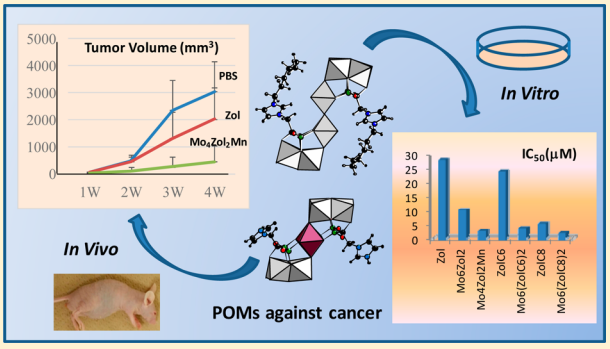

INTRODUCTION

Polyoxometalates (POMs) constitute a class of discrete, anionic, metal−oxygen clusters which can be considered as soluble oxide fragments. They are built from the connection of $\{MO_x\}$ polyhedra, M being a d-block transition metal ion in a high oxidation state, usually W^{VI}, $Mo^{V,VI}$, or $V^{IV,V}$.[1] They can incorporate a large range of organic or inorganic species into their structures. This results in a great variety of sizes, nuclearities, and shapes[2] and a vast range of photochemical,[3] catalytic,[4,5] magnetic[6,7] as well as biological properties including antibacterial,[8] antiviral, and antitumoral activities.[9] POMs can also have activity in tumor cell growth inhibition; e.g., $[NH_3Pr^i]_6[Mo_7O_{24}]\cdot 3H_2O$ exhibits potent antitumor activity against breast, sarcoma, adenocarcinoma, and pancreatic cancer cells.[10] The antitumor activities in vitro of a variety of polyoxotungstates have also been reported, and organometallic derivatives with RSn[11] or CpTi[12] (Cp = cyclopentadienyl) groups appear to be the most efficient. Recently, the cobalt derivative $\{CoSb_6O_4(H_2O)_3[Co(hmta)SbW_8O_{31}]_3\}^{15-}$ (hmta = hexamethylenetetramine) was also shown to kill various cancer cells.[13] Polyoxometalates, in particular, Dawson-type $[P_2Mo_{18}O_{62}]^{6-}$ anions, were also identified as inhibitors of protein kinase CK2, a multifunctional kinase that is deregulated in many cancers.[14]

In order to try to improve activity, one approach is to graft bioactive organic ligands on the inorganic POM core. However, examples of this approach are rare. Organoimido- derivatives of hexamolybdate based on amantadine, an antiviral and anti-Parkinson drug, have been tested in vitro against MCF-7 cells and exhibit better activity than do unfunctionalized hexamolybdate and amantadine.[15] Cholic acid was also grafted onto the

Received: May 3, 2017

DOI: 10.1021/acs.inorgchem.7b01114
Inorg. Chem. XXXX, XXX, XXX−XXX

tris-modified Anderson-type POM $[MnMo_6O_{18}\{(OCH_2)_3CNH_2\}_2]^{3-}$, resulting in enhanced activity over the non-functionalized POM against breast cancer cells (MCF-7, $IC_{50} \approx 56\ \mu M$ and MDA-MB-231, $IC_{50} \approx 38\ \mu M$).[16] A variant of this approach consists of grafting a cleavable group onto a hexamolybdate POM in order to improve degradability with one such hybrid POM being reported to exhibit good activity against human malignant glioma cells (U251, IC50 ≈ 25 μM), the ability to penetrate the blood brain barrier, as well as low toxicity toward rat pheochromocytoma cells (PC12).[17]

In our group, we have been investigating polyoxometalate-bisphosphonate complexes. Bisphosphonates (BPs) having the general formula $H_2O_3PC(OH)(R)PO_3H_2$ have been used clinically for decades to treat bone resorption diseases, and some of them exhibit antitumor activity.[18] Once deprotonated, BPs can form complexes with Mo, W, or V ions, with nuclearities ranging from 1 to 12.[19] In our first investigation, we reported the anticancer activity of hybrid POM/alendronate (Ale) complexes.[20] The dodecanuclear complex $[(Mo^{VI}_3O_8)_4(Ale)_4]^{8-}$, noted here as $Mo_{12}Ale_4$, had IC_{50} values of ∼10 μM against human breast cancer cells (MCF-7) in vitro. This value represents about 4× the activity of the parent alendronate molecule (i.e., on a per-alendronate basis), indicating a potentiating or synergistic effect. We then extended our study to include zoledronate (Zol; Figure 1), the most potent

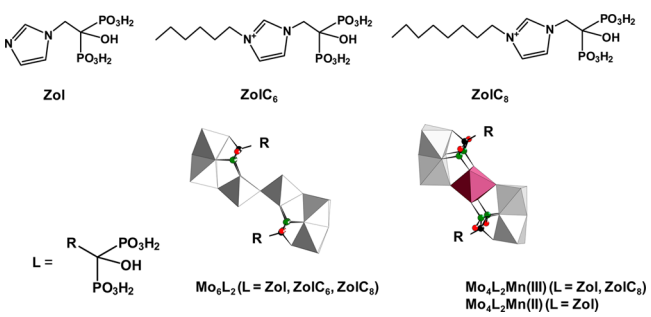

Figure 1. Abbreviations and formulas of the BPs used in this study together with schematic structures of some complexes. Gray polyhedra = MoO_6, purple polyhedron = MnO_6, green spheres = P, black spheres = C, red spheres = O.

commercially available bisphosphonate, and synthesized the hexanuclear complex $[(Mo^{VI}_3O_8)_2O(Zol)_2]^{6-}$.[21] We also investigated the incorporation of a heterometal finding that the most active compound was the Mn(III)-containing POM $[(Mo^{VI}_2O_6)_2(Zol)_2Mn]^{5-}$, also known as $Mo_4Zol_2Mn(III)$, suggesting a possible role for both the heterometal and the BP in growth inhibition.[22]

Here, we describe the synthesis and characterization of a new series of POM/BP complexes and investigate the influence of the oxidation state of the Mn, and the introduction of alkyl chains grafted onto the zoledronate core, on the in vitro activity of these compounds against human nonsmall cell lung cancer (NCI-H460) cells. Lipophilic chains were expected to improve cell uptake of the hybrid POMs since it is known that lipophilic BPs have activities far greater than do nonlipophilic BPs in inhibiting tumor cell growth and invasiveness, both in vitro and in vivo.[23] Furthermore, a recent study revealed that lipophilic zoledronates inhibit both farnesyl and geranylgeranyldiphosphate synthases, effectively blocking prenylation of KRAS and other small G-proteins critical for tumor growth and cell survival.[24] Finally, we report the first results of an in vivo xenograft tumor experiment with a POM/BP/Mn complex.

RESULTS AND DISCUSSION

In order to test the effect of the introduction of a lipophilic chain onto the BP-ligand on tumor cell growth inhibition, two zoledronate-based bisphosphonates, $ZolC_6$ and $ZolC_8$ (Figure 1), were selected for synthesis of Mo/BP complexes. $ZolC_6$ and $ZolC_8$ are zoledronate analogues that have *N*-alkyl chains (n-C_6 or n-C_8) on the unsubstituted nitrogen in the parent zoledronate. These ligands were chosen because they were previously found to be the most active (of Zol analogues containing between 0 and 15 carbon substituents) against a range of tumor cell lines.[24] Two families of complexes were investigated: Mo_6L_2 (L = Zol, $ZolC_6$, $ZolC_8$) or with Mn(III) as the heterometal and with general formulas $Mo_4L_2Mn(III)$ (L = Zol, $ZolC_8$). The structures and ligand abbreviations as well as the structures of all of the complexes reported in this study are shown in Figure 1.

Synthesis and Characterization. Mo_6Zol_2 was synthesized as a reference according to a previously reported procedure.[21] Mo(VI) complexes with lipophilic bisphosphonates were synthesized by reaction of the BP precursor with Mo(VI) ions in aqueous solution at pH ≈ 5. While it was possible to isolate single crystals suitable for X-ray diffraction by slow evaporation of the reaction mixture for $Mo_6(ZolC_6)_2$, only a poorly crystalline powder could be obtained for the $Mo_6(ZolC_8)_2$ complex. However, the similarity of the IR spectra (Figure S1a) and of the ^{31}P NMR spectra (Figure S2) of both compounds, as well as the results of elemental analysis, confirm formation of $Mo_6(ZolC_8)_2$. $Mo_4Zol_2Mn(III)$ was synthesized following a slight modification of the procedure reported previously.[22] $Mo_4Zol_2Mn(II)$ was synthesized by reduction of $Mo_4Zol_2Mn(III)$. Attempts to reduce this complex in solution failed, so its reduction was performed by adding ascorbic acid to a suspension of crystals in methanol, as described for a Mn(III)-containing polyoxotungstate.[25] A color change of the crystals from gray to yellow was observed. This implies that the Mo(VI) centers have not been reduced, because if they were, a blue coloration would be expected. The $\chi_M T$ vs T curve for this compound is shown in Figure S3 where it can be seen that the $\chi_M T$ product is nearly constant between 300 to 50 K ($\chi_M T$ = 4.15 $cm^3\ mol^{-1}\ K$ at 300 K), with a decrease at low temperature ($\chi_M T$ = 2.68 $cm^3\ mol^{-1}\ K$ at 2 K) which can be attributed to the zero-field splitting effect. This indicates that $Mo_4Zol_2Mn(III)$ has been fully reduced to $Mo_4Zol_2Mn(II)$ (at room temperature, the calculated $\chi_M T$ values are 2.94 $cm^3\ mol^{-1}\ K$ for a Mn(III) monomer and 4.29 $cm^3\ mol^{-1}\ K$ for a Mn(II) monomer assuming g = 1.98). As expected, the IR spectra of the oxidized and reduced POMs are very similar (Figure S1b). The synthesis of $Mo_4(ZolC_8)_2Mn(III)$ was performed by reacting $Mn(OAc)_3$ and $ZolC_8$ with a large excess of Na_2MoO_4 in acetate buffer. The reaction with a stoichiometric amount of Mo(VI) ions gave only an insoluble unidentified powder. $Mo_4(ZolC_8)_2Mn(III)$ was characterized by IR spectroscopy (Figure S1c), elemental analysis, and energy dispersive X-ray (EDX) analysis measurements. Despite many attempts, we were unable to isolate the analogous compound with the $ZolC_6$ bisphosphonate.

^{31}P NMR spectroscopy was used to determine whether structures characterized in the solid state were maintained in solution. The ^{31}P NMR spectrum of $Mo_6(ZolC_6)_2$ dissolved in water at room temperature exhibits two singlets at 17.12 and

DOI: 10.1021/acs.inorgchem.7b01114
Inorg. Chem. XXXX, XXX, XXX−XXX

16.82 ppm with relative intensities 0.63:1.37 (Figures 2 and S2a). The same behavior is observed for $Mo_6(ZolC_8)_2$ with two

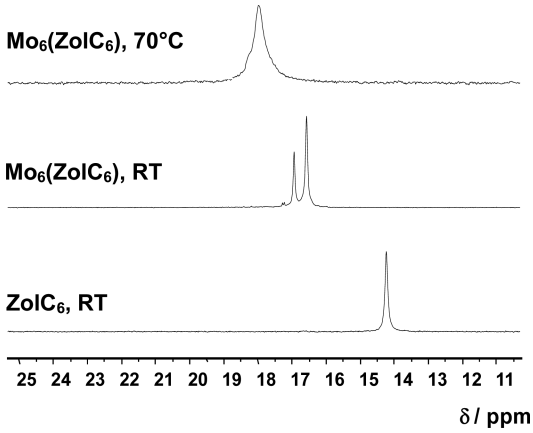

Figure 2. $^{31}P\{^1H\}$ NMR spectra of $Mo_6(ZolC_6)_2$ dissolved in D_2O at two different temperatures and of $ZolC_6$ at room temperature (RT).

singlets at 17.46 and 16.82 ppm with relative intensities 0.89:1.1 (Figure S2b). Only one singlet was expected if the structure observed in the solid state (Figure 3) was retained in solution,

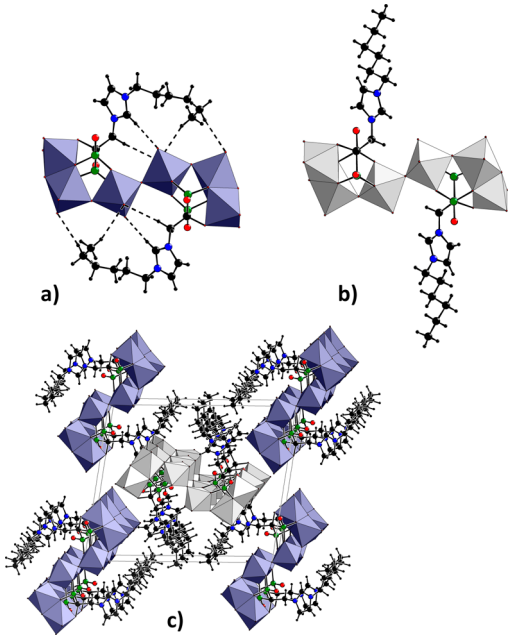

Figure 3. Representation of the two crystallographically independent molecules (a) A and (b) B in the structure of $Mo_6(ZolC_6)_2$. (c) View of the crystal packing. Purple octahedra = MoO_6 octahedra in molecule A, gray octahedra = MoO_6 octahedra in molecule B, green spheres = P, black spheres = C, small black spheres = H, blue spheres = N, red spheres = O, hydrogen bonds are represented as dotted lines.

corresponding to four equivalent phosphorus nuclei. The presence of another singlet close to the first one cannot be attributed to free $ZolC_6$ ligands as the chemical shift of this ligand is equal to 14.45 ppm (Figure 2) and is attributed to an equilibrium between two conformers which differ by the rotation of the two $\{Mo_3O_8\}$ groups around the central oxo bridge (Figure S4).[21] The two resonances are relatively sharp at room temperature and broaden when the temperature increases and finally coalesce at 70 °C (Figure 2), indicating that, as expected, dynamic exchange between the two conformers increases on heating.

We also studied the stability of $Mo_6(ZolC_6)_2$ and $Mo_6(ZolC_8)_2$ under more physiological conditions (0.1 M KH_2PO_4 buffer, pH = 7.4, 0.12 M NaCl, 37 °C) (Figure S2). The ^{31}P NMR spectrum of $Mo_6(ZolC_6)_2$ exhibits two peaks, as observed for the aqueous solution, confirming the stability of the complex. In the spectrum of $Mo_6(ZolC_8)_2$, one of the peaks is split, which may be attributable to the existence of several conformers which could result from different positions of the alkyl chains, as seen in the crystal structure of $Mo_6(ZolC_6)_2$ (vide infra). It can also be seen that the ^1H NMR spectra of $Mo_6(ZolC_8)_2$ in water and in the more physiological conditions are identical (Figure S5).

Structures. The structure of $Mo_6(ZolC_6)_2$ was determined by means of single-crystal X-ray diffraction. There are two crystallographically independent molecules (Figure 3), and the structure of the inorganic core is identical in both molecules. Two $\{Mo_3O_8\}$ trimeric units are connected by a central oxygen atom, and in each trimer Mo(VI) ions are connected to a pentadentate BP ligand by P−O−Mo and C−O−Mo bonds. The six Mo(VI) ions are coplanar, as usually observed for hexanuclear Mo(VI) complexes with BP ligands.[19b] The differences between both complexes lie in the position of the C_6 alkyl chain on the imidazole ring. In one of the molecules (Molecule A, Figure 3a) the chain is bent, and there are short C−H···O distances ($d_{C-H\cdots O}$ in the 2.33−2.80 Å range).[26] In the other molecule (Molecule B, Figure 3b), the alkyl chain is extended away from the cluster. Molecules A and B stack into columns that align in the unit-cell (Figure 3c).

In the Mo_4L_2Mn complexes, IR, elemental analysis, and EDX measurements indicate that the $Mo_4L_2Mn(III)$ (L = Zol, $ZolC_8$) and $Mo_4Zol_2Mn(II)$ complexes have structures that are similar to Mo_4Zol_2Fe.[22] That is, two $\{Mo_2O_6\}$ dimeric units with faced-shared Mo(VI) octahedra are bound to an octahedrally coordinated central Mn ion (Figure 1), and two BP ligands are connected to the Mo and Mn ions through P−O−M and C−O−M (M = Mo, Mn) bonds.

In Vitro and in Vivo Results. We next investigated the effects of the new compounds (together with some compounds reported previously) on tumor cell growth inhibition using the nonsmall cell human lung cancer cell line NCI-H460. Representative dose−response curves are shown in Figure 4 for zoledronate (Figure 4a), $Mo_4Zol_2Mn(II)$ (Figure 4b), $Mo_6(ZolC_6)_2$ (Figure 4c), and $Mo_4(ZolC_8)_2Mn(III)$ (Figure 4d).

IC_{50} values for all compounds are reported in Table 1 on both a molecular weight as well as on a per-bisphosphonate basis. We anticipated that there would be a large increase in activity of the POM/BP complexes containing the more lipophilic bisphosphonates since the lipophilic bisphosphonates acting alone are more active than is zoledronate. With the zoledronate complexes we find that the new $Mo_4Zol_2Mn(II)$ complex has potent activity (on a per bisphosphonate basis), Figure 4b, similar to that of $Mo_4Zol_2Mn(III)$, on average ~6× the activity of zoledronate acting alone and considerably more activity than the Mo_6Zol_2 complex, Table 1. This suggests that the oxidation state of Mn has little influence on the activity of the complex. It can also be seen that zoledronate and the $Mo_4Zol_2Mn(III)$ complex are about 2× more potent in MCF-7 than in NCI-H460 cell lines, as reported previously,[22] reflecting not unexpected cell-to-cell variability. With the $ZolC_6$ system we obtained more activity with the $Mo_6(ZolC_6)_2$ system than

DOI: 10.1021/acs.inorgchem.7b01114
Inorg. Chem. XXXX, XXX, XXX−XXX

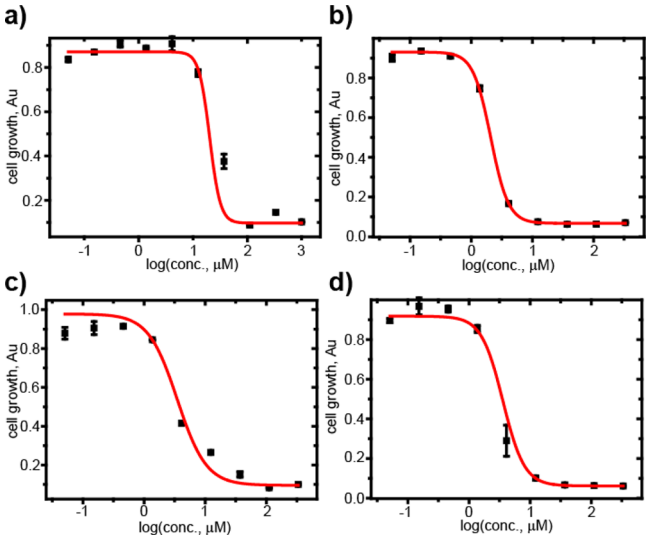

Figure 4. Dose response curves for NCI-H460 cell growth inhibition. (a) Zoledronate. (b) $Mo_4Zol_2Mn(II)$. (c) $Mo_6(ZolC_6)_2$. (d) $Mo_4(ZolC_8)_2Mn(III)$. Three replicates of duplicates were determined, and representative data from one duplicate set are shown.

Table 1. Growth Inhibition of Human Cancer Cell Line NCI-H460 by Bisphosphonates and POM/BP Complexes

formula	IC_{50} [μM]	IC_{50} [μM] per BP	IC_{50} decrease vs BP
Mo_6Zol_2	10 ± 0.9	20 ± 1.8	1.4×
$Mo_4Zol_2Mn(III)$	2.6 ± 0.3	5.2 ± 0.6	5.4×
$Mo_4Zol_2Mn(II)$	2.0 ± 0.1	4.0 ± 0.2	7.0×
Zol	28 ± 3	28 ± 3	1.0×
$Mo_6(ZolC_6)_2$	3.5 ± 0.1	7.0 ± 0.2	3.4×
$ZolC_6$	24 ± 0.8	24 ± 0.8	1.0×
$Mo_6(ZolC_8)_2$	1.9 ± 0.2	3.8 ± 0.4	1.3×
$Mo_4(ZolC_8)_2Mn(III)$	2.9 ± 0.3	5.8 ± 0.6	0.9×
$ZolC_8$	5.1 ± 0.2	5.1 ± 0.2	1.0×

with $ZolC_6$ alone. However, with the more lipophilic $ZolC_8$ species, the activities of all three species: $ZolC_8$, $Mo_6(ZolC_8)_2$, and $Mo_4(ZolC_8)_2Mn(III)$ (Figure 4d) are quite similar to each other as well as to the Mo_4Zol_2Mn complexes, Table 1.

We thus next moved to in vivo studies which since the pioneering work of Yamase and co-workers[10a] have been quite rare.[27] Since there were only small differences in IC_{50} values on a per-bisphosphonate basis between the most active species, we chose to investigate the $Mo_4Zol_2Mn(III)$ species reported earlier in our in vivo study, for the following reasons: (i) it has good activity in both the H460 (lung cancer) cell line described here, as well as against the MCF-7 (breast cancer) cell line reported previously;[22] (ii) zoledronate is commercially available while the alkyl zoledronates require several additional synthesis steps; (iii) zoledronate is already used clinically while the alkyl zoledronates are not; (iv) synthesis of the $Mo_4Zol_2Mn(II)$ complex requires formation of the Mn(III) complex followed by the reduction of the Mn(III) crystals by ascorbate-again an additional synthetic step, and (v) there is little difference in activity between the Mn(II) and Mn(III) complexes, due perhaps to reduction of the latter in cells.

We used the mouse xenograft (SK-ES-1 sarcoma tumor cell growth) model because in previous work we used this system to investigate the effects of lipophilic bisphosphonate chain-length variation on tumor cell growth where we found that a very lipophilic pyridinium analogue of zoledronate (BPH-715, containing an n-C_{10} alkyloxy side-chain) resulted in a ~5× decrease in tumor volume versus zoledronate.[23] Representative results for PBS control, zoledronate, and $Mo_4Zol_2Mn(III)$ treated mice as a function of time are shown in Figures S6a–c, tumor cell volumes as a function of time are shown in Figure S6d, and tumor cell volumes in each of the individual mice after a 4 week treatment are shown in Figure 5a. As can be seen in

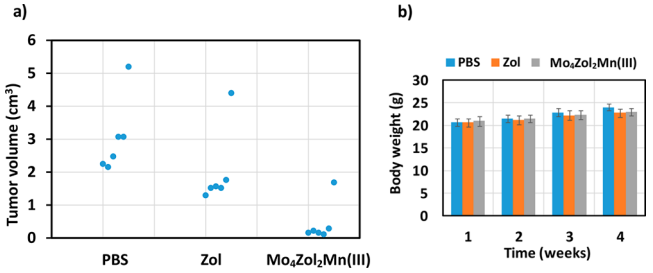

Figure 5. Effects of zoledronate and $Mo_4Zol_2Mn(III)$ on SK-ES-1 tumor volume in 6-week old athymic nude mice treated daily for 28 days with 5 μg compound or phosphate-buffered saline (PBS); 6 mice per group. (a) Tumor volumes in each of the individual mice after a 4 week treatment. (b) Body weights as a function of time for different treatments.

Figures 5a and S6d, there is a very significant (p = 0.045) decrease in tumor cell volume with $Mo_4Zol_2Mn(III)$ dosed at 5 μg/mouse via intratumoral injection once a day for 28 days, corresponding to a ~5× decrease in tumor cell growth versus zoledronate, even though there was only ~1/3 the amount of zoledronate present in the $Mo_4Zol_2Mn(III)$ treatment (due to the high mass of the POM cluster). There is, however, an overlap in the "error bars" between the different treatments. But, as can be seen in Figure 5a, this is due to the presence of just a single "outlier" mouse in each of the three treatments, with 5/6 mice having tumor volumes that are very tightly clustered in each treatment and where, for these points, the reduction in tumor volumes on treatment with $Mo_4Zol_2Mn(III)$ versus zoledronate is rather unambiguous, Figure 5a. There was also only a small difference in mice body weight on zoledronate or $Mo_4Zol_2Mn(III)$ treatment, Figure 5b, showing the absence of any increased toxicity of the complex versus zoledronate alone therapy. These relatively low bisphosphonate concentrations (compared with zoledronate or BPH-715 levels) may make such hybrids in general less toxic than bisphosphonates acting alone, although further work will be needed to investigate this possibility. In the future, it may be possible to carry out detailed structure–activity relationships investigations of these types of complex, although this will be very challenging since it will be necessary to know cell concentrations of the complexes, their stability, as well as the targets for the Mo-moiety as well as the Mn. Plus, as briefly discussed below, both protein prenylation as well as kinase inhibition can be targeted by bisphosphonates.

CONCLUSIONS

We synthesized and characterized four new POM/BP complexes: Mo_6L_2 (L = $ZolC_6$, $ZolC_8$), $Mo_4(ZolC_8)_2Mn(III)$, and $Mo_4Zol_2Mn(II)$, and tested them, together with previously reported analogues, in vitro against a human nonsmall cell lung cancer cell line NCI-H460. The most active compounds had IC_{50} values of ~4–5 μM (on a per-bisphosphonate basis),

DOI: 10.1021/acs.inorgchem.7b01114
Inorg. Chem. XXXX, XXX, XXX–XXX

about 6× more active than zoledronate itself (IC_{50} = 28 μM). One of the most active compounds tested here in vitro was also the most active compound against the MCF-7 breast cancer cell line reported previously, so was investigated in vivo against SK-ES-1 sarcoma cells in a mouse xenograft system. There was a 5-fold decrease in tumor cell volume versus that found with zoledronate after a 28 day treatment period at 5 μg/mouse dosing (~0.2 mg/kg). At present, the molecular basis for the enhanced activity (over that seen with bisphosphonates alone) remains to be determined since both masking of bisphosphonate charge, increasing cell permeability, as well as potentiation of bisphosphonate activity by the (hetero)-polymolybdate moiety may be involved. Nevertheless, the results are of considerable interest because they show for the first time that POM/BP/Mn complexes have potent in vivo activity.

What is particularly attractive about the use of bisphosphonates as ligands in POM complexes is that zoledronate, for example, has the potential for targeting both Ras as well as epidermal growth factor (EGF)-driven tumors. Zoledronate inhibits farnesyl diphosphate synthase and this leads to inhibition of Ras prenylation. Moreover, in two recent articles[28] zoledronate has also been shown to lead to inhibition of EGFR signaling/phosphorylation. It may thus be possible to develop POM-bisphosphonate compounds that target both EGFR as well as Ras-driven cancers. Zoledronate is also an important POM-ligand since zoledronate itself activates gamma-delta T cells (containing the Vγ2 Vδ2 T cell receptor) to kill tumor cells,[29] it switches macrophages from an M2 (tumor promoting) to an M1 (tumor killing) phenotype[30] and inhibits angiogenesis/invasiveness. There are thus good reasons to believe that POM/bisphosphonate/Mn complexes may find utility as drug leads for combination therapies against both Ras as well as EGFR-driven cancers, that also target innate immunity.

EXPERIMENTAL SECTION

Experimental Procedures and Characterization. Zoledronic acid $H_2O_3PC(C_4H_5N_2)(OH)PO_3H_2$ (H_5Zol)[31] and $(NH_4)_6[(Mo_3O_8)_2O(O_3PC(C_4H_6N_2)OPO_3)_2]\cdot 9H_2O$ (Mo_6Zol_2)[21] were synthesized according to reported procedures. $Li_2H_2(ZolC_6)$ and $Li_2H_2(ZolC_8)$ were synthesized with a protocol adapted from literature procedures[24] (see Supporting Information).

Synthesis of $(NH_4)_6[(Mo_3O_8)_2O(O_3PC(C_4H_5N_2)(C_6H_{13})(O)PO_3)_2]\cdot 8H_2O$ ($Mo_6(ZolC_6)_2$). $(NH_4)_6Mo_7O_{24}\cdot 4H_2O$ (0.120 g, 0.10 mmol) was dissolved in 5 mL of 1 M NH_4OAc/HOAc buffer before addition of $Li_2H_2(ZolC_6)$ (0.106 g, 0.24 mmol). The mixture was sealed in a 23 mL Teflon-lined stainless steel reactor before heating to 130 °C over a period of 1 h, kept at this temperature for 20 h, then cooled to room temperature over a period of 36 h. The resulting colorless crystals were collected by filtration. Yield: 0.144 g (68% based on Mo). ^{31}P NMR (300 MHz, D_2O, 25 °C): δ 17.12 (s), 16.76 (s). ^{1}H NMR (300 MHz, D_2O, 60 °C, water saturation): 9.07 (d, 1H, NCHCHN), 7.83 (d, 1H, NCHCHN), 7.63 (s, 1H, NCHN), 5.07 and 4.94 (2m, 2H, NCH_2C), 4.44 (t, 2H, NCH_2CH_2), 2.14 (m, 2H, $NCH_2CH_2CH_2$), 1.59 (m, 6H, CH_2), 1.14 (m, 3H, CH_3). IR (FTR): ν (cm^{-1}) = 1640 (w), 1566 (w), 1433 (vs), 1152 (s), 1127 (s), 1086 (s), 1062 (sh), 1048 (s), 978 (m), 928 (sh), 912 (s), 875 (vs), 730 (vs), 698 (s), 629 (s), 560 (m), 518 (m), 482 (m). Anal. Calc. (found) for $C_{22}H_{76}N_{10}Mo_6O_{39}P_4$ (1804.4 g mol^{-1}): C 14.64 (14.40), H 4.25 (3.99), N 7.76 (7.69). EDX measurements confirm the Mo/P ratio.

Synthesis of $(NH_4)_6[(Mo_3O_8)_2O(O_3PC(C_4H_5N_2)(C_8H_{17})(O)PO_3)_2]\cdot 10H_2O$ ($Mo_6(ZolC_8)_2$). $Na_2MoO_4\cdot 2H_2O$ (0.096 g, 0.40 mmol) was dissolved in 1.5 mL of water (sol. A); $Li_2H_2(ZolC_8)$ (0.055 g, 0.12 mmol) was dissolved in 1.5 mL of water acidified with 2 drops of 1 M hydrochloric acid (sol. B). Sol B was added to sol. A and 1 M HCl was added dropwise to pH = 5. NH_4Cl (0.600 g, 11.3 mmol) was added, resulting in the precipitation of a fine white powder. The mixture was allowed to stir at room temperature for 20 min. The powder was filtered and dried with ethanol and diethyl ether. Yield: 0.061 g (48% based on Mo). ^{31}P NMR (300 MHz, D_2O, 25 °C): δ 17.46 (s), 16.82 (s). ^{1}H NMR (300 MHz, D_2O, 60 °C, water saturation): 9.08 (d, 1H, NCHCHN), 7.86 (d, 1H, NCHCHN), 7.65 (s, 1H, NCHN), 5.05 and 4.96 (m, 2H, NCH_2C), 4.46 (t, 2H, NCH_2CH_2), 2.17 (m, 2H, $NCH_2CH_2CH_2$), 1.61 and 1.56 (m, 10H, CH_2), 1.13 (m, 3H, CH_3). IR (FTR): ν (cm^{-1}) = 1560 (w), 1414 (vs), 1153 (sh), 1134 (s), 1083 (m), 1058 (sh), 1048 (s), 980 (m), 917 (s), 876 (vs), 792 (w), 732 (m), 690 (s), 619 (s), 578 (m), 556 (m), 533 (m), 487 (w), 458 (w). Anal. Calc. (found) for $C_{26}H_{88}N_{10}Mo_6O_{41}P_4$ (1896.5 g mol^{-1}): C 16.47 (16.69), H 4.68 (4.51), N 7.39 (7.36). EDX measurements confirm the Mo/P ratio.

Synthesis of $(NH_4)_5[(Mo^{VI}_2O_6)_2(O_3PC(C_4H_6N_2)OPO_3)_2Mn^{III}]\cdot 10H_2O$ ($Mo_4ZolMn(III)$). To a solution of $Na_2MoO_4\cdot 2H_2O$ (0.242 g, 1 mmol) in 10 mL of 1 M CH_3COONH_4/CH_3COOH buffer was added $Mn(OAc)_3\cdot 2H_2O$ (0.070 g, 0.26 mmol) and zoledronic acid (0.137 g, 0.5 mmol). The solution was stirred for 5 min then NH_3 (33% in water) was added dropwise to pH = 7.5. The solution was left to evaporate and was filtered after 24 h in order to remove a pink precipitate. EDX measurements and IR spectroscopy indicated that the precipitate was a BP complex that did not contain molybdenum. An homogeneous gray crystalline phase of the title compound appeared after 3 days (see picture in Figure S7). Yield: 0.080 g (21% based on Mo). Anal. Calc. (found) for $C_{10}H_{52}MnMo_4N_9O_{36}P_4$ (1437.2 g mol^{-1}): C 8.36 (8.88), H 3.65 (3.90), N 8.77 (8.78). IR (FTR): ν (cm^{-1}) = 1575(m), 1546 (w), 1421(s), 1288 (w), 1136(s), 1112(sh), 1045(s), 1018(sh), 973(m), 915(s), 888(s), 790(s), 699(m), 656(m), 619(w), 560(w), 529(m). EDX measurements confirm the Mo/P and Mo/Mn ratios.

Synthesis of $(NH_4)_5(H_3O)[(Mo^{VI}_2O_6)_2(O_3PC(C_4H_6N_2)OPO_3)_2Mn^{II}]\cdot 6H_2O\cdot 4CH_3OH$ ($Mo_4ZolMn(II)$). Ascorbic acid (0.150 g, 0.85 mmol) was added to a suspension of $Mo_4ZolMn(III)$ (0.190 g, 0.13 mmol) in 30 mL of MeOH. The solution was stirred for 6 h and was filtered. The resulting pale yellow solid was washed with MeOH and dried. Yield: 0.129 g (68%). IR (FTIR): ν (cm^{-1}) = 1579(m), 1546 (w), 1418(s), 1286 (w), 1137(s), 1112(sh), 1047(s), 1018(sh), 975(m), 911(s), 887(s), 786(s), 699(m), 659(m), 619(w), 561(w), 529(m), 485(w). Anal. Calc. (found) for $C_{14}H_{63}N_9MnMo_4O_{37}P_4$ (1512.3 g mol^{-1}): C 11.12 (11.02), H 4.20 (3.47), N 8.34 (7.98). EDX measurements confirm the Mo/P and Mo/Mn ratios.

Synthesis of $Li_2(NH_4)_3[(Mo^{VI}_2O_6)_2(O_3PC(C_4H_5N_2)(C_8H_{17})OPO_3)_2Mn^{III}]\cdot 8H_2O$ ($Mo_4(ZolC_8)_2Mn(III)$). $Na_2MoO_4\cdot 2H_2O$ (0.197 g, 0.82 mmol) was dissolved in 5 mL of 1 M NH_4OAc/HOAc and $Mn(OAc)_3.2H_2O$ (0.018 g, 0.048 mmol) was added. A solution of $Li_2H_2(ZolC_8)$ (0.027 g, 0.060 mmol) in 3 mL of H_2O acidified with a few drops of 1 M HCl until dissolution was slowly added. The pH was adjusted to 5.8 with 33% NH_3. The solution was stirred for 2 h and an orange crystalline precipitate which did not contain $ZolC_8$ was removed by filtration. The pH of the solution was equal to 6.1. The solution was left at room temperature for 5 days, and the thin pinkish platelets (see picture in Figure S7) of the title compound were removed by filtration. Yield 0.011 g (23% based on $ZolC_8$). IR (FTIR): ν (cm^{-1}) = 1639(w), 1661(m), 1420(s), 1123(m), 1046(s), 990(w), 912(m), 871(s), 796(w), 743(w), 691(m), 620(m), 661(m). Anal. Calc. (found) for $C_{26}H_{64}Li_2N_7MnMo_4O_{36}P_4$ (1627.3 g mol^{-1}): C 19.19 (19.97), H 3.96 (4.18), N 6.03 (5.80). EDX measurements confirm the Mo/P and Mo/Mn ratios.

Infrared spectra were recorded on a Nicolet 30 ATR 6700 FTIR spectrometer.

Crystal Structure Determination. Single crystal X-ray diffraction data for $Mo_6(ZolC_6)_2$ were collected by using a Bruker Nonius X8 APEX 2 instrument equipped with a CCD bidimensional detector using the monochromatised wavelength λ(Mo Kα) = 0.71073 Å. Absorption corrections were based on multiple and symmetry-equivalent reflections in the data set using the SADABS program[32] based on the method of Blessing.[33] The structure was solved by direct methods and refined by full-matrix least-squares using the SHELX-TL

DOI: 10.1021/acs.inorgchem.7b01114
Inorg. Chem. XXXX, XXX, XXX−XXX

package.[34] NH_4^+ and H_2O could not be distinguished based on the observed electron densities, therefore, all positions were labeled as O and assigned the oxygen atomic diffusion factor. Crystallographic data are given below and the complete data can be found in the cif file CCDC 1547689.

Crystal data for compound $Mo_6(ZolC_6)_2$: $C_{22}H_{36}Mo_6N_4O_{41}P_4$, M = 1712.07 g mol^{-1}, triclinic, space group $P\bar{1}$, a = 8.8527(6) Å, b = 16.8404(11) Å, c = 19.6929(13) Å, α = 81.370(2)°, β = 83.028(2)°, γ = 76.955(2)°, V = 2816.0(3) Å^3, T = 296 K, Z = 2, D_c = 2.019 g cm^{-3}, μ = 1.515 mm^{-1}, GOF = 1.145, final R indices ($I \geq 2\sigma(I)$) R_1 = 0.0406, wR_2 = 0.1191.

Powder X-ray. Powder X-ray diffraction data were obtained on a Bruker D5000 diffractometer using Cu radiation (1.54059 Å). The comparison of the experimental X-ray powder pattern with the powder pattern calculated from the structure solved from single-crystal X-ray diffraction data confirm the homogeneity of $Mo_6(ZolC_6)_2$ (Figure S8).

EDX Measurements. EDX measurements were performed on a JEOL JSM 5800LV instrument.

NMR Measurements. ^{31}P NMR spectra were recorded in 5 mm tubes with ^{1}H decoupling by using a Bruker AC-300 spectrometer operating at 121.5 MHz. ^{31}P chemical shifts were referenced with respect to an external standard, 85% H_3PO_4, using the convention that low-field, paramagnetic, deshielded values are positive (IUPAC δ-scale). For all compounds 15−20 mg of sample was dissolved in D_2O (500 μL). The concentrations thus varied in the 10−30 mM range.

Magnetic Measurements. Magnetic susceptibility measurements were carried out on polycrystalline samples using a Quantum Design MPMS SQUID magnetometer operating in the 300−2 K temperature range and 0−5.5 T. Susceptibility measurements were performed with an applied field of 1000 Oe. Pascal's constants were utilized to estimate diamagnetic corrections, the value in each case being subtracted from the experimental susceptibility data to give the molar magnetic susceptibility (χ_M).

Cell-Growth Inhibition Assays. The human tumor cell line NCI-H460 (nonsmall cell lung cancer) was obtained from the National Cancer Institute and maintained at 100% humidity and 5% CO_2 at 37 °C. Cell growth inhibition assays were carried out as described previously.[20] A broth microdilution method was used to determine the growth inhibition IC_{50} values. Briefly, ~5 × 10^4 cells suspended in 100 μL of DMEM supplemented with 10% fetal bovine serum (FBS), 4.5 g/L glucose and L-glutamine and preserved with 1% penicillin−streptomycin were seeded in 96-well plates (Corning Inc., Corning, NY) and incubated at 37 °C in a 5% CO_2 atmosphere. The cells were incubated with 1000 μM, 333 μM, 111 μM, 37 μM, 12 μM, 4.1 μM, 1.4 μM, 0.46 μM, 0.15 μM, and 0.051 μM of compounds and H_2O as a control for 4 days.[20] Then, an MTT ((3-(4,5-dimethylthiazol-2-yl)-2,5-diphenyltetrazolium bromide) cell proliferation assay (ATCC, Manassas, VA) was performed to obtain dose−response curves. The IC_{50} values of the free BP, Mo_6Zol_2 and Mo_4Zol_2Mn(III), which had been measured in MCF-7 cells in our first studies[21,22] were redetermined here using the same conditions as for the other compounds (Table 1).

In Vivo Tumor Model. Mice experiments were carried out basically as described in Kubo et al.[35] Xenografts of human SK-ES-1 cells were initiated by subcutaneous injections of 1.5 × 10^7 cells into the right flank of four 6-week old athymic nude mice (CLEA, Tokyo, Japan). The mice received daily local injections of bisphosphonates (5 μg, for 28 days), or physiological saline. The smallest and largest diameters of the tumors, were measured weekly. Tumor volumes were calculated using the following formula: volume (mm^3) = (smallest diameter)^2 × (largest diameter)/2. All animal experiments were conducted according to the guidelines of the Institutional Animal Care and Use Committee, and the protocol was approved by the Ethics Committee for Experimental Animals of Hiroshima University. Statistical significance was determined by one-way ANOVA and independent t test, using SPSSl (version 22, IBM); $p < 0.05$ was considered to be significant.

■ ASSOCIATED CONTENT

Supporting Information

The Supporting Information is available free of charge on the ACS Publications website at DOI: 10.1021/acs.inorgchem.7b01114.

Synthesis of $ZolC_6$ and $ZolC_8$, IR and NMR spectra, $\chi_M T = f(T)$ curve for Mo_4Zol_2Mn(II), representation of the A and B conformers of the Mo_6L_2 compounds, pictures of mice treated with PBS, zoledronate or Mo_4Zol_2Mn(III), SEM images of crystals of Mo_4Zol_2Mn(III) and platelets of $Mo_4(ZolC_8)_2Mn$(III), powder X-ray diffraction pattern of $Mo_6(ZolC_6)_2$ (PDF)

Accession Codes

CCDC 1547689 contains the supplementary crystallographic data for this paper. These data can be obtained free of charge via www.ccdc.cam.ac.uk/data_request/cif, or by emailing data_request@ccdc.cam.ac.uk, or by contacting The Cambridge Crystallographic Data Centre, 12 Union Road, Cambridge CB2 1EZ, UK; fax: +44 1223 336033.

■ AUTHOR INFORMATION

Corresponding Authors

*(E.O.) E-mail: eo@chad.scs.uiuc.edu.

*(A.D.) E-mail: anne.dolbecq@uvsq.fr.

ORCID

Anne Dolbecq: 0000-0001-7940-4152

Notes

The authors declare no competing financial interest.

■ ACKNOWLEDGMENTS

This work was supported by Centre National de la Recherche Scientifique, Université de Versailles-Saint-Quentin-en-Yvelines, L'Agence Nationale de la Recherche (Grant ANR-11-BS07-011-01-BIOOPOM), and by the United States Public Health Service (National Institutes of Health Grants GM065307 and CA158191). Flavien Bourdreux, Grégoire Paille, and Tarik Benali are gratefully acknowledged for the NMR measurements, the SEM images and the synthesis of lipophilic bisphosphonates, respectively.

■ REFERENCES

(1) Special issue on polyoxometalates, *Chem. Rev.* **1998**, *98*, 1−390.

(2) Dolbecq, A.; Dumas, E.; Mayer, C. R.; Mialane, P. Hybrid Organic-Inorganic Polyoxometalate Compounds: From Structural Diversity to Applications. *Chem. Rev.* **2010**, *110*, 6009.

(3) Walsh, J. J.; Bond, A. M.; Forster, R. J.; Keyes, T. E. Hybrid Polyoxometalate Materials for Photo(electro-)chemical Applications. *Coord. Chem. Rev.* **2016**, *306*, 217.

(4) Wang, S.-S.; Yang, G.-Y. Recent Advances in Polyoxometalate-Catalyzed Reactions. *Chem. Rev.* **2015**, *115*, 4893.

(5) Lv, H.; Geletii, Y. V.; Zhao, C.; Vickers, J. W.; Zhu, G.; Luo, Z.; Song, J.; Lian, T.; Musaev, D. G.; Hill, C. L. Polyoxometalate Water Oxidation Catalysts and the Production of Green Fuel. *Chem. Soc. Rev.* **2012**, *41*, 7572.

(6) Zheng, S.-T.; Yang, G.-Y. Recent Advances in Paramagnetic-TM-Substituted Polyoxometalates (TM = Mn, Fe, Co, Ni, Cu). *Chem. Soc. Rev.* **2012**, *41*, 7623.

(7) Clemente-Juan, J. M.; Coronado, E.; Gaita-Ariño, A. Magnetic Polyoxometalates: From Molecular Magnetism to Molecular Spintronics and Quantum Computing. *Chem. Soc. Rev.* **2012**, *41*, 7464.

(8) Yang, P.; Lin, Z.; Bassil, B. S.; Alfaro-Espinoza, G.; Ullrich, M. S.; Li, M.-X.; Silvestru, C.; Kortz, U. Tetra-Antimony(III)-Bridged 18-Tungsto-2-Arsenates(V), $[(LSb^{III})_4(A\text{-}\alpha\text{-}As^{V}W_9O_{34})_2]^{10-}$ (L = Ph,

DOI: 10.1021/acs.inorgchem.7b01114
Inorg. Chem. XXXX, XXX, XXX−XXX

OH): Tuning Bioactivity On and Off by Ligand Substitution. *Inorg. Chem.* **2016**, *55*, 3718.
(9) (a) Yamase, T. Anti-tumor, -viral, and -bacterial Activities of Polyoxometalates for Realizing and Inorganic drug. *J. Mater. Chem.* **2005**, *15*, 4773. (b) Hasenknopf, B. Polyoxometalates: Introduction to a Class of Inorganic Compounds and their Biomedical Applications. *Front. Biosci., Landmark Ed.* **2005**, *10*, 275.
(10) (a) Yamase, T.; Fujita, H.; Fukushima, K. Medical chemistry of polyoxometalates. Part1. Potent Antitumor Activity of Polyoxomolybdates on Animal Transplantable Tumors and Human Cancer Xenograft. *Inorg. Chim. Acta* **1988**, *151*, 15. (b) Ogata, A.; Mitsui, S.; Yanagie, H.; Kasano, H.; Hisa, T.; Yamase, T.; Eriguchi, M. A Novel Anti-tumor Agent, Polyoxomolybdate Induces Apoptotic Cell Death in AsPC-1 Human Pancreatic Cancer Cells. *Biomed. Pharmacother.* **2005**, *59*, 240.
(11) Wang, X. H.; Dai, H. C.; Liu, J. F. Synthesis and Characterization of Organotin-Substituted Heteropolytungstosilicates and their Biological Activity. *Polyhedron* **1999**, *18*, 2293.
(12) Wang, X.; Liu, J.; Li, J.; Yang, Y.; Liu, J.; Li, B.; Pope, M. T. Synthesis and Antitumor Activity of Cyclopentadienyltitatinium Substituted Polyoxotungstate $[CoW_{11}O_{39}(CpTi)]^{7-}$ (Cp = *eta*^{5}-C_5H_5). *J. Inorg. Biochem.* **2003**, *94*, 279.
(13) Zhang, Z.-M.; Duan, X.; Yao, S.; Wang, Z.; Lin, Z.; Li, Y.-G.; Long, L.-S.; Wang, E.-B.; Lin, W. Cation-Mediated Optical Resolution and Anticancer Activity of Chiral Polyoxometalates Built from Entirely Achiral Building Blocks. *Chem. Sci.* **2016**, *7*, 4220.
(14) Prudent, R.; Moucadel, V.; Laudet, B.; Barette, C.; Lafanechère, L.; Hasenknopf, B.; Li, J.; Bareyt, S.; Lacôte, E.; Thorimbert, S.; Malacria, M.; Gouzerh, P.; Cochet, C. Identification of Polyoxometalates as Nanomolar Noncompetitive Inhibitors of Protein Kinase CK2. *Chem. Biol.* **2008**, *15*, 683.
(15) She, S.; Bian, S.; Hao, J.; Zhang, J.; Zhang, J.; Wei, Y. Aliphatic Organoimido Derivatives of Polyoxometalates Containing a Bioactive Ligand. *Chem. - Eur. J.* **2014**, *20*, 16987.
(16) Yang, H.-K.; Cheng, Y.-X.; Su, M.-M.; Xiao, Y.; Hu, M.-B.; Wang, W.; Wang, Q. Polyoxometalate-Biomolecule Conjugates: a New Approach to Create Hybrid Drugs for Cancer Therapeutics. *Bioorg. Med. Chem. Lett.* **2013**, *23*, 1462.
(17) She, S.; Bian, S.; Huo, R.; Chen, K.; Huang, Z.; Zhang, J.; Hao, J.; Wei, Y. Degradable Organically-Derivatized Polyoxometalate with Enhanced Activity Against Glioblastoma Cell Line. *Sci. Rep.* **2016**, *6*, 33529.
(18) (a) Singh, A. P.; Zhang, Y.; No, J.-H.; Docampo, R.; Nussenzweig, V.; Oldfield, E. Lipophilic Bisphosphonates Are Potent Inhibitors of Plasmodium Liver-Stage Growth. *Antimicrob. Agents Chemother.* **2010**, *54*, 2987. (b) Mukherjee, S.; Huang, C.; Guerra, K.; Wang, K.; Oldfield, E. Thermodynamics of Bisphosphonates Binding to Human Bone: a Two-Site Model. *J. Am. Chem. Soc.* **2009**, *131*, 8374. (c) Zhang, Y.; Cao, R.; Yin, F.; Lin, F. Y.; Wang, H.; Krysiak, K.; Mukkamala, D.; Houlihan, K.; Li, J.; Morita, C. T.; Oldfield, E.; No, J.-H. Lipophilic Pyridinium Bisphosphonates: Potent Gamma Delta T Cell Stimulators. *Angew. Chem., Int. Ed.* **2010**, *49*, 1136. (d) Song, Y.; Lin, F. Y.; Yin, F.; Hensler, M.; Rodrigues Poveda, C. A.; Mukkamala, D.; Cao, R.; Wang, H.; Morita, C. T.; Gonzalez Pacanowska, D.; Nizet, V.; Oldfield, E. Phosphonosulfonates are Potent, Selective Inhibitors of Dehydrosqualene Synthase and Staphyloxanthin Biosynthesis in Staphylococcus Aureus. *J. Med. Chem.* **2009**, *52*, 976. (e) Zhang, Y.; Hudock, M. P.; Krysiak, K.; Cao, R.; Bergan, K.; Yin, F.; Leon, A.; Oldfield, E. Activity of Sulfonium Bisphosphonates on Tumor Cell Lines. *J. Med. Chem.* **2007**, *50*, 6067. (f) Clézardin, P. Bisphosphonates' Antitumor Activity: an Unravelled Side of a Multifaceted Drug Class. *Bone* **2011**, *48*, 71.
(19) (a) Banerjee, A.; Bassil, B. S.; Röschenthaler, G.-V.; Kortz, U. Diphosphates and Diphosphonates in Polyoxometalate Chemistry. *Chem. Soc. Rev.* **2012**, *41*, 7590. (b) Dolbecq, A.; Mialane, P.; Sécheresse, F.; Keita, B.; Nadjo, L. Functionalized Polyoxometalates with Covalently Linked Bisphosphonate, N-donor or Carboxylate Ligands: from Electrocatalytic to Optical Properties. *Chem. Commun.* **2012**, *48*, 8299.
(20) Compain, J.-D.; Mialane, P.; Marrot, J.; Sécheresse, F.; Zhu, W.; Oldfield, E.; Dolbecq, A. Tetra- to Dodecanuclear Oxomolybdate Complexes with Functionalized Bisphosphonate Ligands: Activity in Killing Tumor Cells. *Chem. - Eur. J.* **2010**, *16*, 13741.
(21) El Moll, H.; Zhu, W.; Oldfield, E.; Rodriguez-Albelo, L. M.; Mialane, P.; Marrot, J.; Vila, N.; Mbomekallé, I.-M.; Rivière, E.; Duboc, C.; Dolbecq, A. Polyoxometalates Functionalized by Bisphosphonate Ligands: Synthesis, Structural, Magnetic, and Spectroscopic Characterizations and Activity on Cell Lines. *Inorg. Chem.* **2012**, *51*, 7921.
(22) Saad, A.; Zhu, W.; Rousseau, G.; Mialane, P.; Marrot, J.; Haouas, M.; Taulelle, F.; Dessapt, R.; Serier-Brault, H.; Rivière, E.; Kubo, T.; Oldfield, E.; Dolbecq, A. Polyoxometalate Bisphosphonate Heterometallic Complexes: Synthesis, Structure and Activity on a Breast Cancer Cell Line. *Chem. - Eur. J.* **2015**, *21*, 10537.
(23) Zhang, Y.; Cao, R.; Yin, F.; Hudock, M. P.; Guo, R. T.; Krysiak, K.; Mukherjee, S.; Gao, Y. G.; Robinson, H.; Song, Y.; No, J. H.; Bergan, K.; Leon, A.; Cass, L.; Goddard, A.; Chang, T. K.; Lin, F. Y.; Beek, E. V.; Papapoulos, S.; Wang, A. H.; Kubo, T.; Ochi, M.; Mukkamala, D.; Oldfield, E. Lipophilic Bisphosphonates as Dual Farnesyl/Geranygeranyl Diphosphate Synthase Inhibitors: an X-ray and NMR Investigation. *J. Am. Chem. Soc.* **2009**, *131*, 5153.
(24) Xia, Y.; Liu, Y.-L.; Xie, Y.; Zhu, W.; Guerra, F.; Shen, S.; Yeddula, N.; Fischer, W.; Low, W.; Zhou, X.; Zhang, Y.; Oldfield, E.; Verma, I. M. A Combination Therapy for KRAS-Driven Lung Adenocarcinomas Using Lipophilic Bisphosphonates and Rapamycin. *Sci. Transl. Med.* **2014**, *6*, 263ra161.
(25) Thiel, J.; Ritchie, C.; Streb, C.; Long, D.-L.; Cronin, L. Heteroatom-Controlled Kinetics of Switchable Polyoxometalate Frameworks. *J. Am. Chem. Soc.* **2009**, *131*, 4180.
(26) Taylor, R.; Kennard, O. Crystallographic Evidence for the Existence of C-H···O, C-H···N, and C-H···C1 Hydrogen-Bonds. *J. Am. Chem. Soc.* **1982**, *104*, 5063.
(27) See for example (a) Sun, T.; Cui, W.; Yan, M.; Qin, G.; Guo, W.; Gu, H.; Liu, S.; Wu, Q. Target Delivery of a Novel Antitumor Organoplatinum(IV)-Substituted Polyoxometalate Complex for Safer and More Effective Colorectal Cancer Therapy In Vivo. *Adv. Mater.* **2016**, *28*, 7397. (b) Dong, Z.; Tan, R.; Cao, J.; Yang, Y.; Kong, C.; Du, J.; Zhu, S.; Zhang, Y.; Lu, J.; Huang, B.; Liu, S. Discovery of Polyoxometalate-based HDAC Inhibitors with Profound Anticancer *In Vitro* and *In Vivo*. *Eur. J. Med. Chem.* **2011**, *46*, 2477. (c) Wang, X.; Li, F.; Liu, S.; Pope, M. T. New Liposome-encapsulated-polyoxometalates: Synthesis and Antitumoral Activity. *J. Inorg. Biochem.* **2005**, *99*, 452.
(28) (a) Yuen, T.; Stachnik, A.; Iqbal, J.; Sgobba, M.; Gupta, Y.; Lu, P.; Colaianni, G.; Ji, Y.; Zhu, L.-L.; Kim, S.-M.; Li, J.; Liu, P.; Izadmehr, S.; Sangodkar, J.; Bailey, J.; Latif, Y.; Mujtaba, S.; Epstein, S.; Davies, T. F.; Bian, Z.; Zallone, A.; Aggarwal, A. K.; Haider, S.; New, M. I.; Sun, L.; Narla, G.; Zaidi, M. Bisphosphonates Inactive Human EGFRs to Exert Antitumor Actions. *Proc. Natl. Acad. Sci. U. S. A.* **2014**, *111*, 17989. (b) Stachnik, A.; Yuen, T.; Iqbal, J.; Sgobba, M.; Gupta, Y.; Lu, P.; Colaianni, G.; Ji, Y.; Zhu, L.-L.; Kim, S.-M.; Li, J.; Liu, P.; Izadmehr, S.; Sangodkar, J.; Scherer, T.; Mujtaba, S.; Galsky, M.; Gomez, J.; Epstein, S.; Buettner, C.; Bian, Z.; Zallone, A.; Aggarwal, A. K.; Haider, S.; New, M. I.; Sun, L.; Narla, G.; Zaidi, M. Repurposing of Biphosphonates for the Prevention and Therapy of Nonsmall Cell Lung and Breast Cancer. *Proc. Natl. Acad. Sci. U. S. A.* **2014**, *111*, 17995.
(29) Nada, M. H.; Wang, H.; Workalemahu, G.; Tanaka, Y.; Morita, C. T. Enhancing Adoptive Cancer Immunotherapy with Vγ2Vδ2 T Cells through Pulse Zoledronate Stimulation. *J. Immunother. Cancer.* **2017**, *5*, doi: 10.1186/s40425-017-0209-6.
(30) Coscia, M.; Quaglino, E.; Iezzi, M.; Curcio, C.; Pantaleoni, F.; Riganti, C.; Holen, I.; Mönkkönen, H.; Boccadoro, M.; Forni, G.; Musiani, P.; Bosia, A.; Cavallo, F.; Massaia, M. Zoledronic acid repolarizes tumour-associated macrophages and inhibits mammary carcinogenesis by targeting the mevalonate pathway. *J. Cell. Mol. Med.* **2010**, *14*, 2803.
(31) Martin, M. B.; Grimley, J. S.; Lewis, J. C.; Heath, H. T., III; Bailey, B. N.; Kendrick, H.; Yardley, V.; Caldera, A.; Lira, R.; Urbina, J.

DOI: 10.1021/acs.inorgchem.7b01114
Inorg. Chem. XXXX, XXX, XXX−XXX

A.; Moreno, S. N. J.; Docampo, R.; Croft, S. L.; Oldfield, E. Bisphosphonates Inhibit the Growth of *Trypanosoma Brucei*, *Trypanosoma Cruzi*, Leishmania Donovani, *Toxoplasma Gondii*, and *Plasmodium Falciparum*: a Potential Route to Chemotherapy. *J. Med. Chem.* **2001**, *44*, 909.
(32) Sheldrick, G. M. *SADABS, Program for Scaling and Correction of Area Detector Data*; University of Göttingen: Germany, 1997.
(33) Blessing, R. An Empirical Correction for Absorption Anisotropy. *Acta Crystallogr., Sect. A: Found. Crystallogr.* **1995**, *51*, 33.
(34) Sheldrick, G. M. *SHELX-TL version 5.03, Software Package for the Crystal Structure Determination*; Siemens Analytical X-ray Instrument Division: Madison, WI USA, 1994.
(35) Kubo, T.; Shimose, S.; Matsuo, T.; Tanaka, K.; Yasunaga, Y.; Sakai, A.; Ochi, M. Inhibitory Effects of a New Bisphosphonate, Minodronate, on Proliferation and Invasion of a Variety of Malignant Bone Tumor Cells. *J. Orthop. Res.* **2006**, *24*, 1138.

DOI: 10.1021/acs.inorgchem.7b01114
Inorg. Chem. XXXX, XXX, XXX−XXX